

INTERNATIONAL SOCIETY FOR SOIL MECHANICS AND GEOTECHNICAL ENGINEERING



This paper was downloaded from the Online Library of the International Society for Soil Mechanics and Geotechnical Engineering (ISSMGE). The library is available here:

<https://www.issmge.org/publications/online-library>

This is an open-access database that archives thousands of papers published under the Auspices of the ISSMGE and maintained by the Innovation and Development Committee of ISSMGE.

Assessment of soil liquefaction during earthquakes

Évaluation de la liquéfaction de sol pendant les tremblements de terre

D.S.Liyanapathirana – *The University of Sydney, Australia*
 H.G.Poulos – *Coffey Geosciences Pty Ltd & The University of Sydney, Australia*

ABSTRACT: This paper presents a new method for assessing the liquefaction potential of a soil deposit subjected to an earthquake loading. In most of the currently available methods of assessing liquefaction potential, the nature of the earthquake and the dissipation of the pore water pressure during the shaking are not taken into account. In the method presented, the nature of the earthquake is included in the parameter V which is the gross area under the input acceleration record. By analysing 15 earthquake records from different parts of the world, a method is outlined to assess the effects of the dissipation of pore water pressures and the nature of the earthquake on the liquefaction potential.

RÉSUMÉ: Cet article présente une nouvelle méthode pour évaluer le potentiel de liquéfaction d'un dépôt de sol soumis à un chargement de tremblement de terre. Dans la plupart des méthodes actuellement disponibles d'évaluer le potentiel de liquéfaction, la nature du tremblement de terre et la dissipation de la pression d'eau interstitielle pendant la secousse ne sont pas prises en considération. Dans la méthode présentée, la nature du tremblement de terre est incluse dans le paramètre V qui est la zone brute sous l'enregistrement d'accélération d'entrée. En analysant 15 enregistrements de tremblement de terre de différentes régions du monde, une méthode est tracée les grandes lignes pour évaluer les effets de la dissipation des pressions d'eau interstitielle et de la nature du tremblement de terre sur le potentiel de liquéfaction.

1 INTRODUCTION

When saturated sand deposits are subjected to earthquake-induced shaking, pore water pressures are built up leading to liquefaction or loss of soil strength. Major earthquakes that have occurred during past years such as the 1964 Niigata and the 1995 Hyogoken-Nambu demonstrated the damaging effects of soil liquefaction. Therefore it is necessary to develop simplified methods to assess the liquefaction potential in designing earthquake-resistant structures and in seismic microzonation for environmental planning.

Most earthquakes occur around the boundaries of the tectonic plates such as earthquakes that occur in California, USA. The Australian continent is in the middle of one of the world's largest tectonic plates and therefore subject to relatively low earthquake activity. However, the 1989 Newcastle earthquake has increased the awareness of the need to properly assess the possible consequences of earthquakes.

Although Australian earthquakes have high acceleration levels, evidence of liquefaction has not been reported. The major difference between Californian and Australian earthquakes is that in Australian earthquakes, high acceleration levels last only a few seconds while in Californian earthquakes, high acceleration levels may exist during almost the whole duration of the earthquake.

Although methods are available to assess the risk of liquefaction during an earthquake, they generally do not consider the nature of the earthquake or the reduction in liquefaction potential due to dissipation of pore water pressures during shaking. The main objective of this paper is to outline a procedure that takes into account the above factors in assessing liquefaction potential of a soil deposit.

2 NUMERICAL MODEL

The numerical model used in the ground response analyses presented in what follows is based on a one-dimensional finite

element model. Equations of the motion were integrated directly using the constant average acceleration method and the soil behaviour is modelled using a hyperbolic stress-strain relationship.

The initial maximum values of shear modulus G_0 and shear strength τ_0 of the soil are defined using the equations given by Hardin and Drnevich (1972) as shown below:

$$G_0 = 14760 \frac{(2.973 - e)^2}{1 + e} \sqrt{\left(\frac{1 + 2K_0}{3}\right) \frac{\sigma'_{v_0}}{47.9}} * 47.9 \quad (1)$$

$$\tau_0 = \sqrt{\left(\frac{1 + K_0}{2} \sin \phi'\right)^2 - \left(\frac{1 - K_0}{2}\right)^2} \sigma'_{v_0} \quad (2)$$

where, e is the void ratio of the soil, K_0 is the coefficient of earth pressure at rest, ϕ' is the effective angle of shearing resistance and σ'_{v_0} is the initial effective vertical stress. Both G_0 and τ_0 are given in N/m^2 .

Generation of pore water pressures during earthquake shaking was calculated using the method proposed by Seed *et al.* (1976). According to this method, the undrained rate of pore pressure generation is given by,

$$\frac{\partial u_g}{\partial t} = \frac{\sigma'_{v_0}}{\alpha \pi N_l \sin^{2\alpha-1} \left(\frac{\pi u_g}{2 \sigma'_{v_0}}\right) \cos \left(\frac{\pi u_g}{2 \sigma'_{v_0}}\right) \frac{\partial N}{\partial t}} \quad (3)$$

$$\frac{\partial N}{\partial t} = \frac{N_{eq}}{t_d} \quad (4)$$

where u_g is the generated pore water pressure if the drainage is

prevented, σ'_{vo} is the effective vertical stress, t_d is the duration of the earthquake, α is a coefficient which depends on the test condition and soil properties, N_{eq} is the number of uniform stress cycles of the earthquake at each depth having an amplitude of $0.65 \tau_{max}$ developed during the earthquake. This number is calculated based on the method proposed by Seed *et al.* (1975). N_i is the number of cycles required to cause liquefaction when the stress level is equal to $0.65 \tau_{max}$.

Since the earthquake motion induces periods of high stress intensity followed by periods of little activity, the number of equivalent cycles of the earthquake is calculated by dividing the duration of the earthquake into number of periods.

The overall distribution of excess pore water pressure in the deposit is calculated by taking into account the pore pressure dissipation due to consolidation.

To calculate N_{eq} , initially a non-linear analysis is carried out neglecting any pore pressure effects. After that, an effective stress analysis is carried out by taking into account the generation and dissipation of pore water pressures in the soil deposit during each time step of the calculation.

3 LIQUEFACTION POTENTIAL

The degree of severity of each scaled earthquake can be assessed by the liquefaction potential index I_L defined by Iwasaki *et al.* (1984) as shown below:

$$I_L = \int_0^{20} FW(z) dz \quad (5)$$

where $F = 1 - F_L$ for $F_L \leq 1.0$, $F = 0$ for $F_L > 1.0$, $W(z) = 10 - 0.5z$ and z is the depth in metres.

F_L is the factor of safety against liquefaction and defined as:

$$F_L = \frac{R}{S_s} \quad (6)$$

where R is the in-situ cyclic undrained shear strength of the soil mobilised for N_{eq} number of cycles, N_{eq} is the number of equivalent cycles of the earthquake and S_s is the $0.65 \tau_{max}$ due to the earthquake.

Iwasaki *et al.* (1984) proposed the following simplified procedure to assess soil liquefaction in a particular site.

Table 1. Liquefaction risk assessment (Iwasaki *et al.*, 1984).

Liquefaction risk	
$I_L = 0$	very low
$0 < I_L \leq 5$	low
$5 < I_L \leq 15$	high
$15 < I_L$	very high

4 EFFECT OF NATURE OF THE EARTHQUAKE ON LIQUEFACTION POTENTIAL

To study the effect of the nature of the earthquake on the liquefaction potential, acceleration records of 15 earthquakes that have occurred during the past 60 years in different parts of the world were analysed. In currently available simplified methods, when calculating liquefaction potential, τ_{max} is calculated based on the maximum acceleration at the ground surface neglecting the nature of the earthquake. Here, the nature of the earthquake is included in the parameter V which is given by,

$$V = \int_0^{t_d} |acc| dt \quad (7)$$

where, t_d is the duration of the earthquake and acc is the acceleration at time t .

If Figures 1 and 2 are compared, the main difference between intra-plate earthquakes in Australia and earthquakes along plate boundaries such as those occur in California, can be seen. Although Australian earthquakes have high acceleration levels, they last only a few seconds.

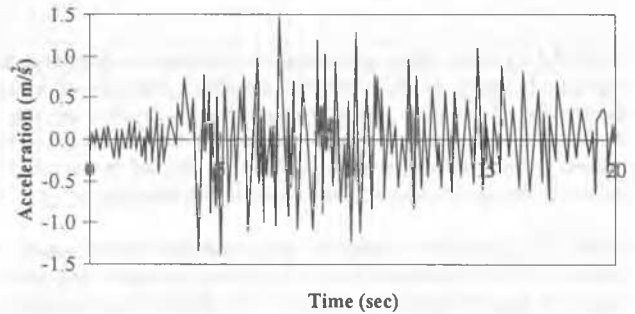


Figure 1. Acceleration record of Taft earthquake (California, 1966) scaled to 0.15g.

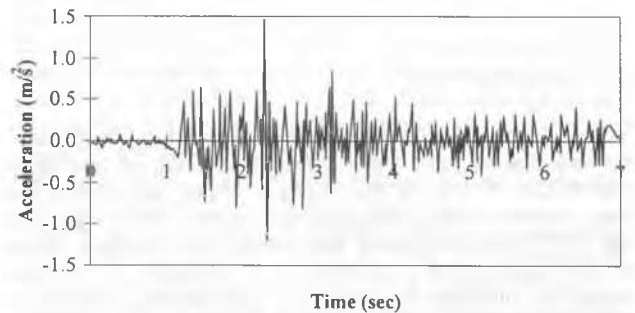


Figure 2. Base input motion of Meckering Earthquake (Western Australia, 1968) scaled to 0.15g.

Table 2. V values for the earthquakes used for the study.

Name of Earthquake	V (max. acc. 0.1g)
New Zealand - 1973	2.36
New Zealand - 1991	1.07
San Fernando	3.05
Northridge	2.89
Oolong	0.44
Taft	3.95
Gunjung	1.53
Tenant Creek	0.32
Meckering	0.66
Cadoux	0.19
Newcastle - 1989	2.29
Newcastle - 1994	2.13
Pasadena	7.33
Melendy Ranche	0.51
El-Centro	4.11

Table 2 summarises the V values obtained for earthquakes used for this study, scaled to maximum acceleration of 0.1g. All Australian earthquakes except Newcastle earthquakes, scaled to 0.1g, have very low V values compared to inter-plate earthquakes such as San Fernando, Northridge, Taft, Pasadena and El-Centro.

Table 3. Values of parameters used for the analysis.

Input Parameters	
Density (kg/m ³)	1900
K_0	0.6
e	0.6
α	1.3
ϕ'	40°
Dr %	55
Coef. of vol. Compressibility (at low pore p.) - m_v (m ² /N)	2x10 ⁻⁸
Water table (m)	13.5

To illustrate the effect of V on liquefaction potential, a 15 m deep soil deposit with properties as given in Table 3 is subjected to the earthquakes listed in Table 2 scaled to acceleration levels 0.1g, 0.15g and 0.2g. It is assumed that the soil behaves as undrained. Figure 3 shows the variation in I_L with V . It can be seen that there is a critical V , beyond which I_L starts to increase with V . If the variation in maximum excess pore pressure generated in the soil deposit is studied, it can be seen that beyond the critical V , the maximum pore pressure is 1.0 and when V is less than critical V , the maximum pore pressure generated in the deposit has an almost linear variation with V . This can be seen in Figure 4.

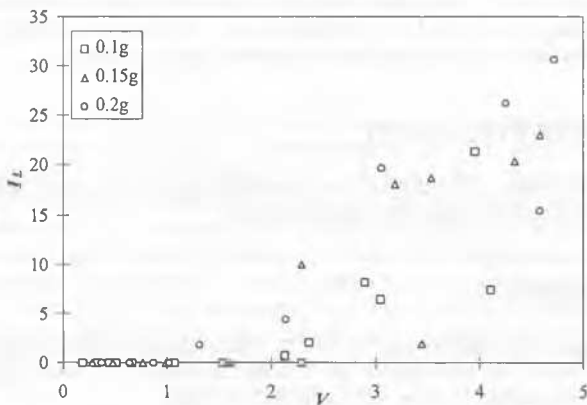


Figure 3. Variation of I_L with V

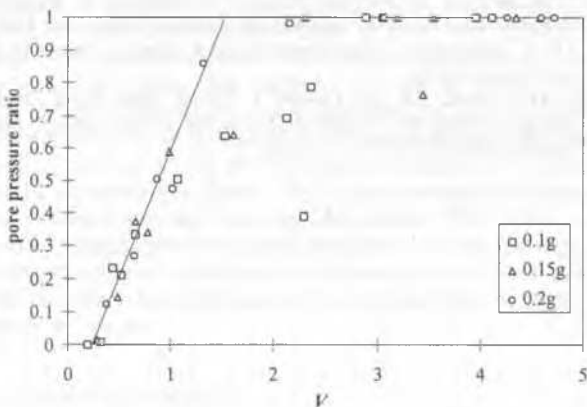


Figure 4. Variation of pore pressure ratio with V

If the analysis is repeated for several relative densities, it can be seen that each relative density has a different critical V . Figure 5 shows the I_L values corresponding to different V when Dr varies from 45% to 90%. A chart like this is very useful in assessing I_L for a soil deposit when the input acceleration

record and the relative density of the soil is known.

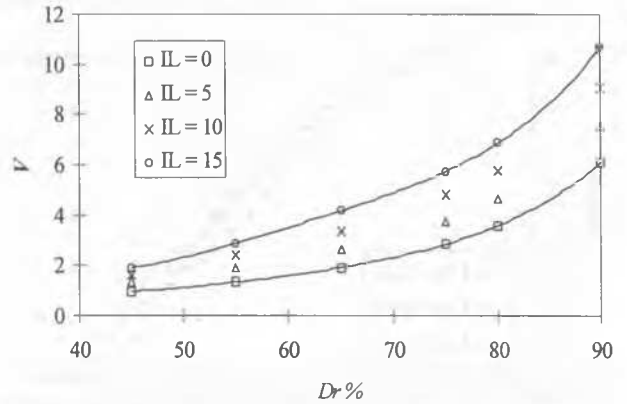


Figure 5. Variation in Liquefaction potential with critical V and relative density (Dr %)

According to Figures 3 and 4, it is clear that liquefaction potential is very low when V is relatively low. Except for the Newcastle earthquakes, all Australian earthquakes have very low V values. As a result, there appears to be a low risk of liquefaction in Australia.

5 EFFECT OF PERMEABILITY ON LIQUEFACTION POTENTIAL

In most of the currently available methods of assessing liquefaction potential, the effect of permeability, k , of the soil is not considered but it has a significant effect on the pore pressure generated in the soil deposit. Figure 6 shows the maximum pore pressure ratio developed in the 15 m soil deposit. It can be seen that when k increased from 10^{-3} to 10^{-2} m/s, maximum pore pressure in the soil deposit has reduced by about 50%. If the maximum cyclic shear stress generated in the soil deposit is compared for the different permeabilities as in Figure 7, it can be seen that they are nearly the same. This would suggest the same I_L for all three cases. However the maximum pore pressure ratio has reduced from 1.0 to 0.5, and according to Figures 3 and 4, when the maximum pore pressure ratio is 0.5, I_L is nearly zero. Hence the liquefaction risk should be very low if the pore pressure dissipation is taken into consideration. Therefore it is important to include effect of pore pressure dissipation in calculating the risk of liquefaction.

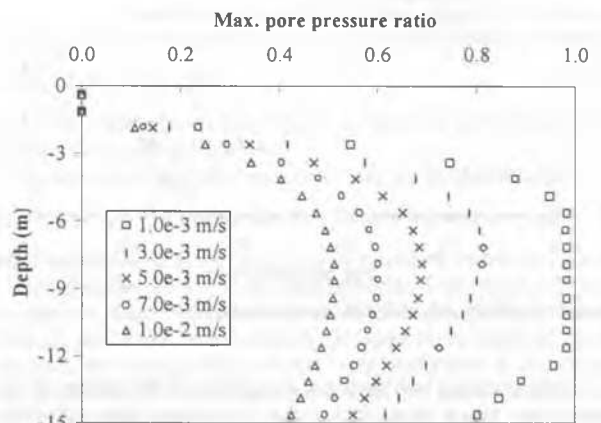


Figure 6. Maximum pore pressure generated along the depth with different permeabilities.

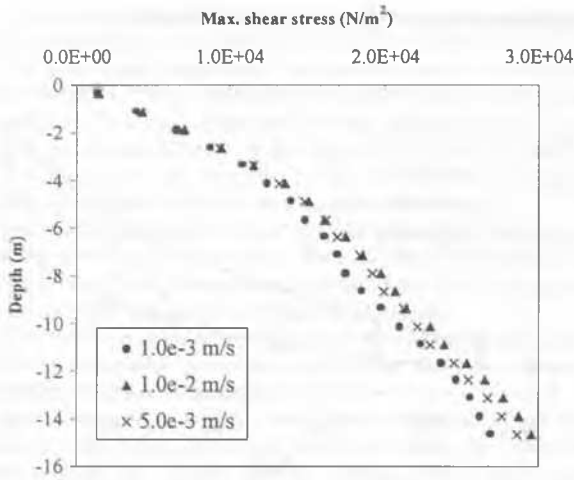


Figure 7. Maximum shear stress along depth after including pore pressure generation and dissipation effects.

6 ASSESSMENT OF I_L USING V AND k

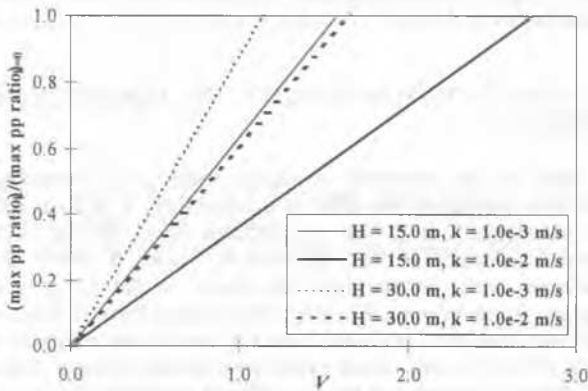


Figure 8. $(\max. \text{pp ratio})/(\max. \text{pp ratio})_{k=0}$ when the depth of the deposit is 15 m and 30 m.

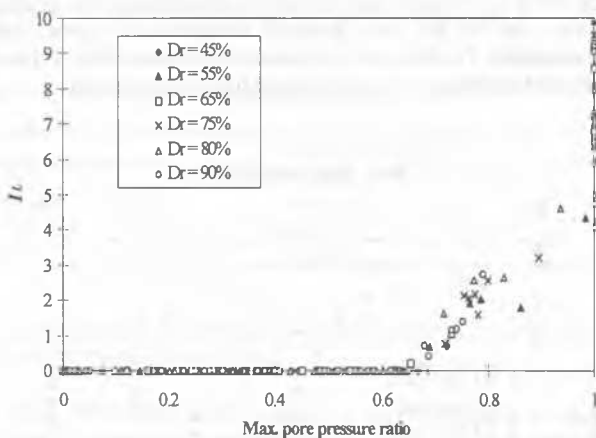


Figure 9. Variation in I_L with max. pore pressure ratio.

In the previous two sections, the effects of the nature of the earthquake on I_L and k on the maximum pore pressure generated in the soil deposit have been studied. Using a chart like Figure 8, the reduction in pore pressure due to dissipation can be assessed for a range of permeabilities. For the same earthquake record, when the depth of the deposit is increased,

$(\max \text{ pp ratio})_k/(\max \text{ pp ratio})_{k=0}$ increases due to reduction in maximum pore pressure ratio under undrained conditions. In this chart, the nature of the earthquake is included via V .

Figure 9 shows the variation in I_L with maximum pore pressure ratio generated in the soil deposit for several relative densities. It can be seen that there is a nearly unique relationship between I_L and the maximum pore pressure ratio, irrespective of the relative density of the soil. After obtaining the reduction in maximum pore pressure ratio in the soil deposit using a chart like Figure 8, liquefaction potential can be assessed using a chart like Figure 9.

7 CONCLUSIONS

A method is presented to assess the effects of pore pressure dissipation and the nature of the earthquake on the liquefaction potential. By analysis of 15 earthquake records at different maximum acceleration levels, it was shown that when V is relatively low, liquefaction risk is low. Although dissipation of pore pressure reduces liquefaction risk, it does not change the maximum cyclic shear stress induced. Hence the methods currently used in practise cannot predict the effect of soil permeability on liquefaction potential. A chart is given for 15 m and 30 m soil deposits to assess the reduction in maximum pore pressure generated in the soil deposit due to increase in k when V is known. Using the relationship between maximum pore pressure ratio and I_L presented, the reduced liquefaction potential due to pore pressure dissipation can be assessed.

ACKNOWLEDGEMENT

This project is funded by the Australian Research Council and this support is gratefully acknowledged.

REFERENCES

- Hardin, B.O. and Drnevich, V.P. (1972). "Shear Modulus and Damping in Soils: Design Equations and Curves." *Journal of Soil Mech. and Foundation Division*, ASCE, 98:SM7, 667-692
- Iwasaki, T., Arakawa, T. and Tokida, K.I. (1984). "Simplified Procedures for Assessing Soil Liquefaction During Earthquakes." *Soil Dyn. and Earthq. Eng.*, 3:1, 49-58
- Seed, H.B., Idriss, I.M., Makdisi, F. and Banerjee, N. (1975). "Representation of Irregular Stress Time Histories by Equivalent Uniform Stress Series in Liquefaction Analyses." *Report No. EERC 75-29, Earthquake Engineering Research Centre, University of California, Berkeley.*
- Seed, H.B., Martin, P.P. and Lysmer, J. (1976). "Pore Water Pressure Changes During Soil Liquefaction." *Journal of the Geotech. Eng. Division*, ASCE, 102:GT4, 323-346.